

# Superoleophobic Textured Copper Surfaces Fabricated by Chemical Etching/Oxidation and Surface Fluorination

Junfei Ou,<sup>†</sup> Weihua Hu,<sup>†</sup> Sheng Liu,<sup>‡</sup> Mingshan Xue,<sup>\*,†</sup> Fajun Wang,<sup>†</sup> and Wen Li<sup>\*,†</sup>

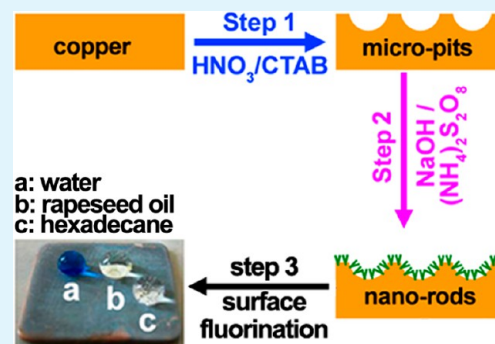
<sup>†</sup>School of Materials Science and Engineering, Nanchang Hangkong University, Nanchang 330063, P. R. China

<sup>‡</sup>Zibo City Institute of New Materials, Zibo 255040, P. R. China

## Supporting Information

**ABSTRACT:** We report a convenient route to fabricate superoleophobic surfaces (abridged as SOS) on copper substrate by combining a two-step surface texturing process (first, the substrate is immersed in an aqueous solution of HNO<sub>3</sub> and cetyltrimethyl ammonium bromide, and then in an aqueous solution of NaOH and (NH<sub>4</sub>)<sub>2</sub>S<sub>2</sub>O<sub>8</sub>) and succeeding surface fluorination with 1H,1H,2H,2H-perfluorodecanethiol (PFDT) or 1-decanethiol. The surface morphologies and compositions were characterized by field emission scanning electron microscopy and X-ray diffraction, respectively. The results showed that spherical micro-pits (SMP) with diameter of 50–100 μm were formed in the first step of surface texturing; in the second step, Cu(OH)<sub>2</sub> or/and CuO with structures of nanorods/microflowers/microballs were formed thereon. The surface wettability was further assessed by optical contact angle meter by using water (surface tension of 72.1 mN m<sup>-1</sup> at 20°C), rapeseed oil (35.7 mN m<sup>-1</sup> at 20°C), and hexadecane (25.7 mN m<sup>-1</sup> at 20°C) as probe liquids. The results showed that, as the surface tension decreasing, stricter choosing of surface structures and surface chemistry are required to obtain SOS. Specifically, for hexadecane, which records the lowest surface tension, the ideal surface structures are a combination of densely distributed SMP and nanorods, and the surface chemistry should be tuned by grafted with low-surface-energy molecules of PFDT. Moreover, the stability of the so-fabricated sample was tested and the results showed that, under the testing conditions, superhydrophobicity and superoleophobicity may be deteriorated after wear/humidity resistance test. Such deterioration may be due to the loss of outermost PFDT layer or/and the destruction of the above-mentioned ideal surface structures. For UV and oxidation resistance, the sample remained stable for a period of 10 days.

**KEYWORDS:** copper, superoleophobicity, composite structures, stability



## 1. INTRODUCTION

Superhydrophobicity and superoleophobicity, which display high static contact angle (SCA, >150°) and low sliding angle (SA) with different probe liquids (such as water and low surface tension liquids) on surfaces,<sup>1</sup> has found wide application in daily life and various sectors of national production due to its characteristics of self-cleaning,<sup>2</sup> anti-freezing,<sup>3</sup> anti-sticking of snow,<sup>4</sup> anti-corrosion,<sup>5–8</sup> anti-biofouling,<sup>9</sup> etc. Such wide potential application has stimulated many researchers to fabricate superhydrophobic surfaces (abridged as SHS) by anodization,<sup>10</sup> electrodeposition,<sup>11</sup> laser treating,<sup>12</sup> electrospinning,<sup>13</sup> chemical vapor deposition<sup>14</sup> etc. However, compared with these intensive researches on SHS, the fabrication of superoleophobic surfaces (abridged as SOS) is difficult and related reports are rare.<sup>1,15</sup>

The difficulty in obtaining SOS can be well understood by the following theoretical analyses. According to Wenzel model, the SCA increases with the increase of surface roughness when the SCA of a liquid on a flat surface is larger than 90°.<sup>16</sup> However, it is difficult to get SCA greater than 90° for low surface tension liquids on a flat surface. This is because that the SCA ( $\theta$ ) on a flat surface is determined by Young's eq 1

$$\cos \theta = \frac{\gamma_s - \gamma_{sl}}{\gamma_l} \quad (1)$$

where  $\gamma_s$ ,  $\gamma_l$ , and  $\gamma_{sl}$  are the surface tension of solid, liquid, and the interfacial tension of solid/liquid, respectively. The interfacial tension  $\gamma_{sl}$  can be shown as eq 2

$$\gamma_{sl} = \gamma_l + \gamma_s - 2\sqrt{\gamma_l \gamma_s} \quad (2)$$

By combining the above two equations and the term of  $\theta = 90^\circ$ , it is obtained  $\gamma_s = \gamma_l/4$ .<sup>17</sup> The  $\gamma_l$  of low surface tension liquids is usually in the range of 20–30 mN m<sup>-1</sup>, so the value of  $\gamma_s$  is several mN · m<sup>-1</sup>. Such a low  $\gamma_s$  is difficult to obtain, so SOS can not be easily prepared.

However, it has been demonstrated that SOS can be obtained by the introduction of specially designed surface geometries, such as re-entrant and overhang surface structures,<sup>18–24</sup> even with  $\theta < 90^\circ$ . This is consistent with Cassie and Baxter's eq 3<sup>25,26</sup>

Received: June 28, 2013

Accepted: September 27, 2013

Published: September 27, 2013

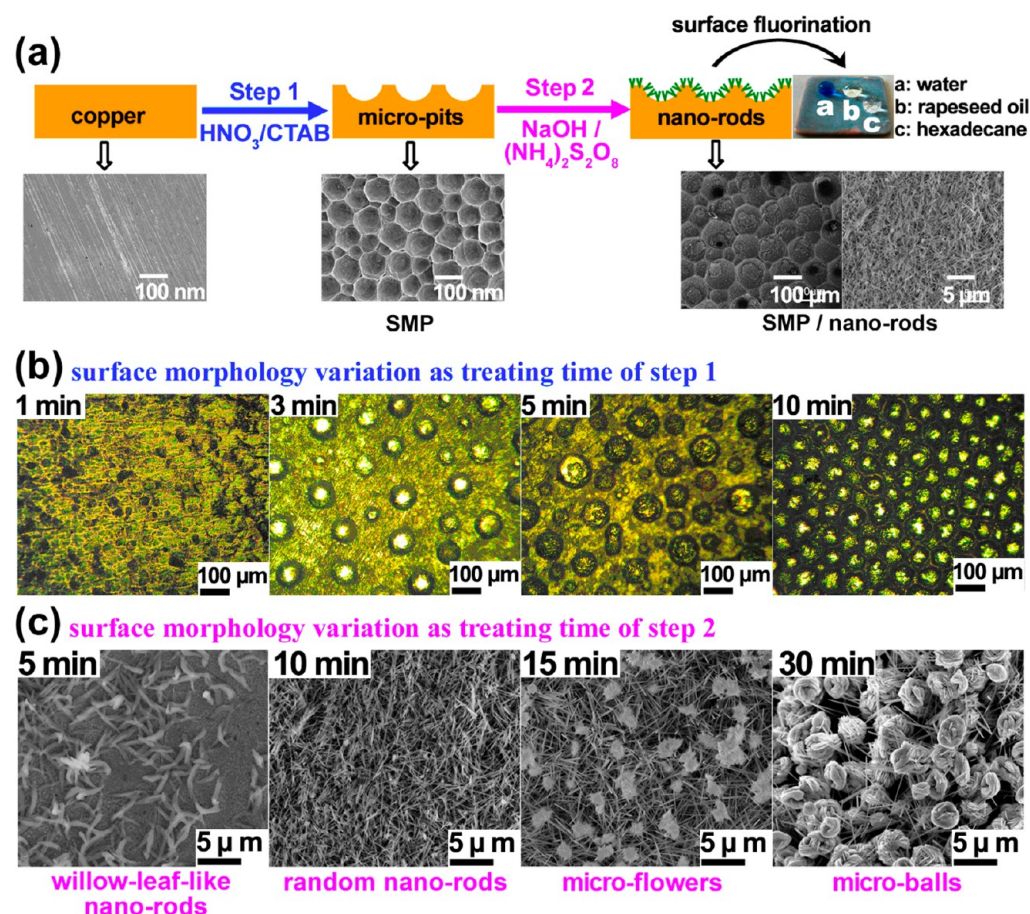


**Figure 1.** (a) Schematic view for the preparation procedure of SOS on copper substrate and the surface morphology variation as treating time of (b) step 1 and (c) step 2. Larger magnification for c can be seen in Supporting Information (Figure 2s).

$$\cos \theta_c = f_1 \cos \theta_1 - f_2 \quad (3)$$

where  $f_1$  is the total area of solid under the drop per unit projected area under the drop,  $\theta_1$  is the contact angle on a smooth surface of material 1. Likewise,  $f_2$  is defined in an analogous way, with material 2 as air ( $\theta_1 = 180^\circ$ ).  $\theta_c$  is the SCA on the rough surface. In contrast to the Wenzel relation, the Cassie relation allows for the possibility of  $\theta_c > 90^\circ$ , even with  $\theta_1 < 90^\circ$  because of air entrapment in the composite state. The composite structures prevent water and low surface tension liquids from penetrating the cavities as a consequence of capillary forces. However, the composite structures have been realized with specific fabrication processes, such as unconventional anodization,<sup>15</sup> dc magnetron sputtering,<sup>27</sup> and conventional photolithographic technique.<sup>28</sup> Herein, we aim to fabricate SOS with simple solution-based technique.

The studied substrate in this work is copper, which is a kind of important engineering metals and widely used in many applications, such as aerospace, railway, and automobiles. The fouling of copper by oil/water pollution are big problems in these fields. To relieve these problems, endowing copper with superoleophobicity is an attractive alternative, because it would inhibit the contact of a surface with oil/water and environmental humidity. In this paper, a two-step process based on simple solution immersion is proposed to fabricate similar surface composite structures on copper substrates. Specifically, by chemical etching in  $\text{HNO}_3/\text{CTAB}$  and chemical oxidizing in  $\text{NaOH}/(\text{NH}_4)_2\text{S}_2\text{O}_8$ , composite structures composed of spherical micropits (SMP)/nanorods were fabricated.<sup>29</sup> After

further surface passivation with low-surface-energy molecules of 1H,1H,2H,2H-perfluorodecanethiol, SOS were fabricated successfully. The treating condition for this process is mild (dilute solution, room temperature, and atmospheric pressure) and the operation is fairly easy; moreover, it needs no special large apparatus. These obvious advantages may accelerate the fabrication of SOS by convenient routes.

## 2. EXPERIMENTAL SECTION

To remove the surface grease, copper substrates (99.7%, Sinopharm Chemical Reagent Co., Ltd) were ground with abrasive paper and ultrasonically cleaned in acetone, ethanol and ultrapure water for 10 min, respectively. Then, the copper substrates were immersed into an aqueous solution containing 5 M  $\text{HNO}_3$  and 1.2 mM CTAB [ $\text{C}_{16}\text{H}_{33}(\text{CH}_3)_3\text{NBr}$ , 90%, Sinopharm Chemical Reagent Co., Ltd] under ultrasonication at room temperature for a period of time to fabricate microstructures, followed by rinsing with a great deal of ultrapure water and drying with nitrogen.<sup>22</sup> After this, the copper substrates were immersed in an aqueous solution of 2.5 M NaOH and 0.1 M  $(\text{NH}_4)_2\text{S}_2\text{O}_8$  at room temperature ( $27^\circ\text{C}$ ) to obtain nanostructures, followed by rinsing with a great deal of ultrapure water and drying with nitrogen.<sup>23</sup> After the composite structures were formed, surface fluorination was performed in an ethanol solution (1.0 wt %) of PFDT (1H,1H,2H,2H-perfluorodecanethiol, 97%, Sigma-Aldrich) or DT (1-decanethiol, 96%, Alfa Aesar) at room temperature for 60 min, subsequently rinsing with ultrapure water, and drying with nitrogen.

Static contact angle (SCA) and sliding angle (SA) were measured by a contact angle meter (Easydrop, Krüss, Germany) at room temperature with 4  $\mu\text{L}$  probe liquids of water, rapeseed oil, and



hexadecane. Surface morphologies were observed on field-emission scanning electron microscope (FESEM, Nova NanoSEM, FEI, USA). Surface compositions were characterized by an X-ray diffraction meter (XRD, Bruker-axs, D8ADVANCE, Germany) and X-ray photoelectron spectroscopy (XPS, Physical Electronics, PHI-5702, USA). The stability, including wear/humidity/UV resistance/oxidation, of the so-fabricated sample was also tested, and the conditions for testing were listed in Figure 4. No special apparatus was needed except for UV resistance (ZN-P).

### 3. RESULTS AND DISCUSSION

**3.1. Surface structures and compositions.** To further reveal the composition variation after such a two-step process,

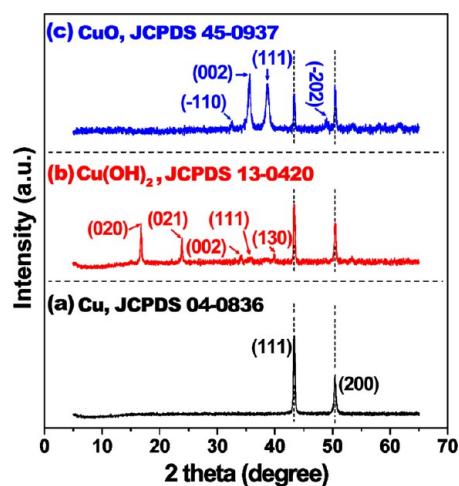
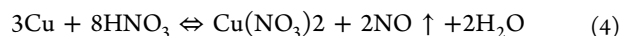
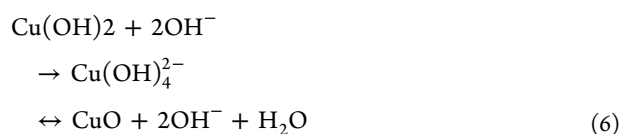
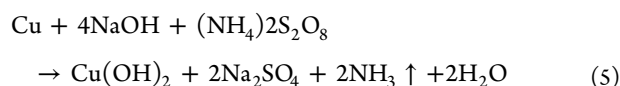


**Figure 2.** XRD patterns of copper substrate (a) treated by step 1 and (b, c) further treated by step 2 for (b) 10 and (c) 30 min.

we depicted XRD patterns of copper substrate treated by step 1 and step 2 in Figure 2a. It is observed that, after treated by step 1, the substrate displays two main peaks at  $2\theta = 43.3$  and  $50.4^\circ$ , which can be ascribed to the (111) and (200) crystalline planes of Cu, respectively. This suggests that there deposit no new species on the substrate by step 1. This can be well-understood if one consults the following reaction equation



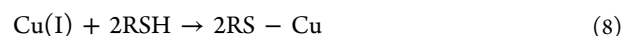
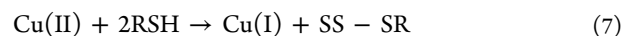
the product of such a etching reaction is dissolvable  $\text{Cu}(\text{NO}_3)_2$ , NO gas, and water; no new species are deposited on the substrate. After treated by step 2, the copper is supposed to be oxidized into copper hydroxide (for immersion time of 5 or 10 min) or further into cupric oxide (for immersion time of 30 min) by the following reaction equations:<sup>30</sup>



consequently, new peaks attributed to the undissolvable  $\text{Cu}(\text{OH})_2$  (Figure 2a-ii) or CuO (Figure 2a-iii) appeared.

After the rough structures were formed, PFDT was used to lower the surface energy. The self assembling of alkanethiol on copper has been widely studied; however, on oxidized copper

surface, the reports are rare.<sup>31–33</sup> These pioneer works<sup>32,33</sup> show that Cu (II) species can be reduced by alkanethiol to  $\text{Cu}_2\text{O}$  (eq 7), which can further react with alkanethiol to form a self assembled monolayer (eqs 8 or 9).



These reactions can be regarded as the anchoring mechanism of PFDT on the oxidized rough copper substrate.

**3.2. Surface Wettability.** The surface wettability is mainly controlled by two aspects, viz., the probe liquid and the tested surface. As to the former, in our present work, water, rapeseed oil, and hexadecane was used; the reported surface tension of these probe liquids is 72.1, 35.7, and 25.7  $\text{mN m}^{-1}$  ( $20^\circ\text{C}$ ),<sup>15</sup> respectively. As to the latter, it also includes two aspects, viz., surface structures and surface chemistry. For a given probe liquid, to obtain a special wettability of superhydrophobicity or superoleophobicity, rough surface structures and low surface energy is generally required. Herein, rough surface structures are fabricated by a single step (step 1 or step 2) or by a combination of two steps (Figure 1a); the low surface energy is obtained by grafting with PFDT or DT. The influence of these parameters, viz., the surface structures and the grafted low-energy molecules, on surface wettability was studied.

**3.2.1. Influence of Surface Structures on Wettability.** It is widely reported that special surface structures (i.e., micro-/nanocomposite structures) are required to fabricate SHS/SOS. Moreover, for different probe liquids, such combination of micro-structures and nano-structures may be different. Specifically, for probe liquid with lower surface tension, stricter combination is generally required. Herein, “stricter” means that both microstructures and nanostructures should be obvious. For example, by fabricating well-ordered nanowires on microstructured aluminum surface, SOS to diverse liquids (including water, hexadecane, etc.) has been obtained;<sup>15</sup> for the aluminum surface with obvious microstructures and not so obvious nanostructures, only SHS can be obtained.<sup>34</sup>

On the basis of these analyses, it is expected that the surface structures suitable for hexadecane SOS are most difficult to obtain in the present work because of its lowest surface tension (as discussed earlier). To discover such proper surface structures for different probe liquids, especially for hexadecane, we studied a series of surface structures were fabricated by controlling the treating time for step 1/step 2 and wettability, and the results were summarized in Figure 3. It is observed that the variation of SCA on the treating time is different for different probe liquids. Specifically, for water (the upper blue curve in Figure 3), after the substrate was treated by step 2 (see Figure 3a) or step 1 (see “0 min for step 2” in Figure 3a–e) solely, SCA increased gradually as the treating time prolonging and SHS can be easily prepared when a critical time reaches. The conditions for SHS can be expressed simply as follows

SHS: step 1 (10 min) or step 2 ( $x$  min,  $x = 10, 15, 30$ )

For step 1 (10 min), microstructures (i.e., densely-distributed SMP) with not obvious nanostructures (i.e., nano irregular papillae) are generated;<sup>7</sup> for step 2 (10 min), random nanorods are generated (Figure 1c), the typical size of which is in nano-scale, while the random distribution lead to a microstructures; for step 2 (15 min) and step 2 (30 min), microflowers with

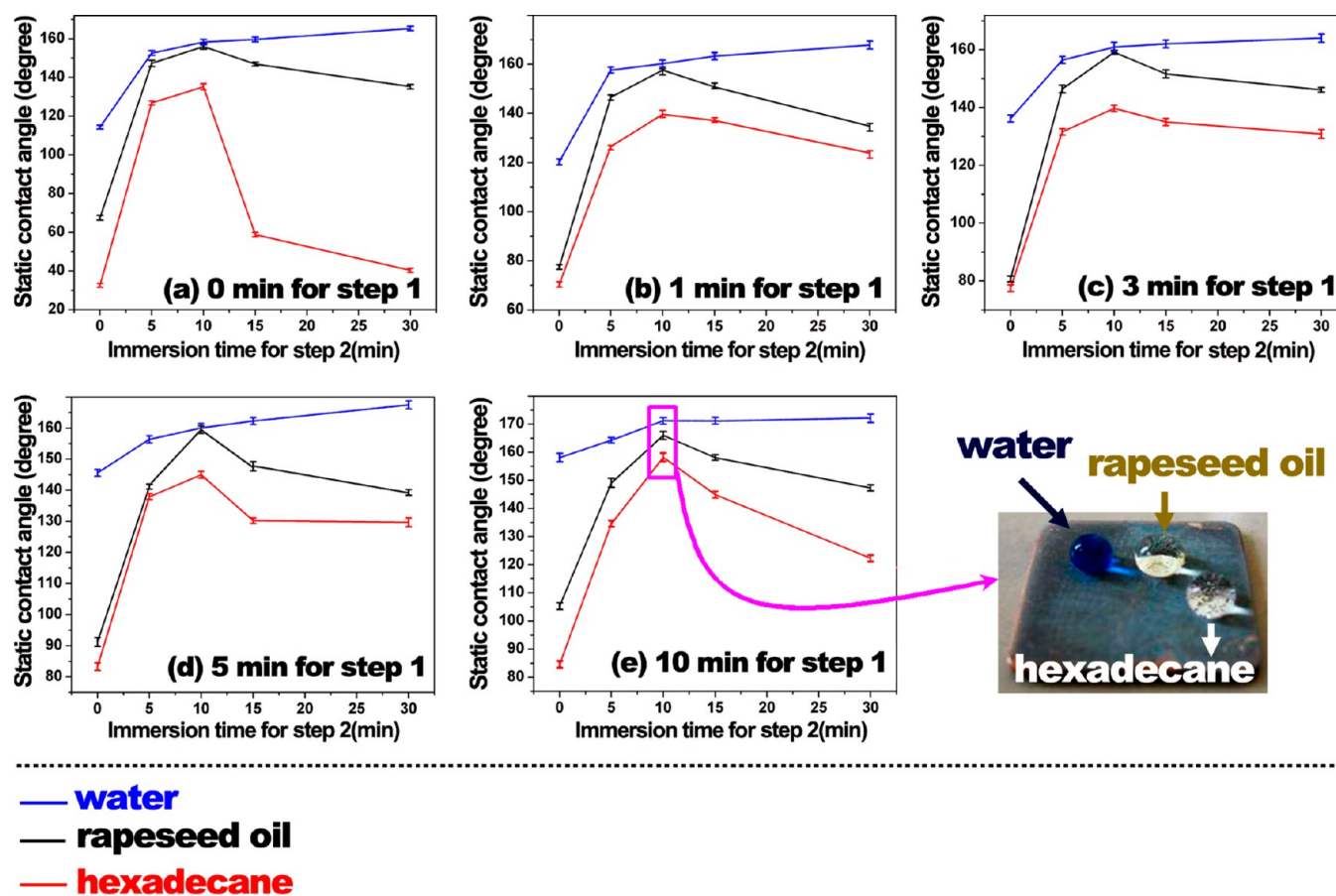


**Figure 3.** Relationship between the immersion time and SCA with different probe liquids. The rough surfaces are grafted with PFDT. When SCA is larger than  $150^\circ$ , SA is also tested. For water, SA is less than  $10^\circ$  when a SCA is larger than  $150^\circ$ ; for rapeseed oil and hexadecane, the highest SCA and corresponding SA values in a–e are shown in Table 1.

**Table 1.** SCA/SA Values for the Peak Points in Figure 3 for Rapeseed Oil and Hexadecane

	SCA/SA Value (deg)				
	Figure 3a	Figure 3b	Figure 3c	Figure 3d	Figure 3e
rapeseed oil	$156.0 \pm 1.4$ $20 \pm 4$	$157.5 \pm 2.0$ $20 \pm 3$	$159.2 \pm 1.2$ $18 \pm 4$	$159.5 \pm 2.0$ $17 \pm 3$	$166.1 \pm 2.2$ $15 \pm 2$
hexadecane	$135.15 \pm 1.6$ 90	$139.6 \pm 1.6$ 90	$141.1 \pm 1.0$ 90	$145.0 \pm 1.4$ 90	$158.2 \pm 2.6$ $20 \pm 3$

nanorods and microballs with nanorods are generated, respectively. SHS can be easily obtained on these composite structures, even for some surfaces, the nanostructures (step 1 (10 min)) or microstructures (step 2 (10 min)) are not so obvious.

For rapeseed oil (the middle black curve in Figure 3) and hexadecane (the lower red curve in Figure 3), there exists a peak point (10 min for step 2) in the curves. By referring to the corresponding SEM image (Figure 1 c, 10 min for step 2), it is apparent that nanorods are generated. Such nanorods are supposed to be the factors to enhance the oleophobicity, and this enhancement can be well understood if one notices that the oleophobicity is obtained by repulsing the low surface tension liquids (i.e., rapeseed oil and hexadecane) from the spaces among neighboring nanorods ( $r$ ) via capillary pressure ( $\Delta p$ ), which can be expressed as<sup>35</sup>

$$\Delta p = 2\gamma \cos \theta / r \quad (d)$$

where  $\theta$  is the contact angle and  $\gamma$  surface tension of the liquid. The repulsing capillary pressure is very obvious when the spaces are in nanoscale (see Figure 2sb in the Supporting Information); consequently, oleophobicity or superoleophobicity was obtained. For rapeseed oil, all such peak points are greater than  $150^\circ$ ; however, for hexadecane, only peak point in Figure 3e (step 1 (10 min) and step 2 (10 min)) is greater than  $150^\circ$ . The necessary conditions to fabricate SOS can be expressed simply as follows

$$\begin{aligned} \text{SOS for rapeseed oil: step 1} & (x \text{ min}, x \\ & = 0, 1, 3, 5, 10) \text{ and step 2 (10 min)} \end{aligned}$$

$$\text{SOS for hexadecane: step 1 (10 min) and step 2 (10 min)}$$

It is obvious that, the condition to obtain SOS for hexadecane is strictest. Under such condition, both micro-structures (i.e., densely distributed SMP) and nanostructures (nanorods) are obvious. The combination of such micro-/nanostructures leads

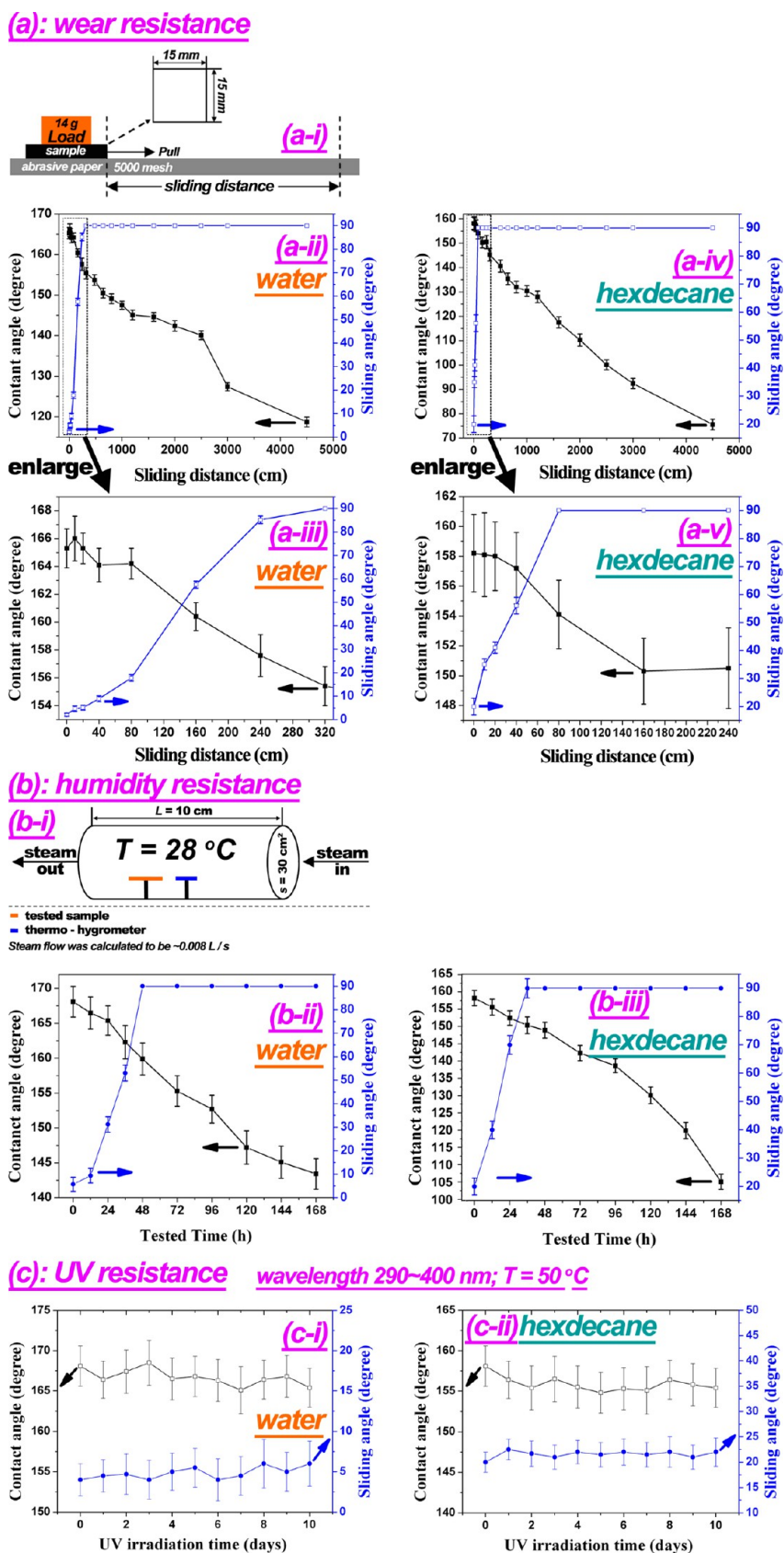


**Figure 4.** (a-i), (b-i) Schematic view for the devices used to estimate the stability, and the wear/humidity/UV resistance for the sample obtained by step 1 (10 min)/step 2 (10 min). The probe liquid for (a-ii), (a-iii), (b-ii), and (c-i) is water; for others, the probe liquid is hexdecane.

to superoleophobicity. Comparatively, for rapeseed oil, the combination can be more arbitrary: even step 2 (10 min) solely

can produce SOS; for water, both step 2 and step 1 are effective in producing SHS. So, it can be concluded that as the surface



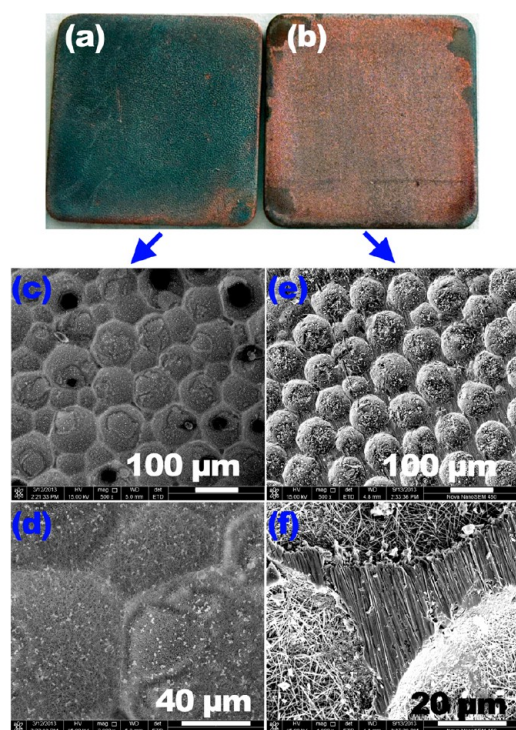


**Figure 5.** Digital and SEM images for the sample obtained by step 1 (10 min)/step 2 (10 min) (a, c, d) before and (b, e, f) after sliding for 4500 cm.

tension decreases, the fabrication of SHS or SOS becomes more and more difficult. In other words, as the surface tension decreases, more accurate surface structures are needed to generate superoleophobicity.

**3.2.2. Influence of Surface Chemistry on Wettability.** For the surface structures obtained under the treating time of step 1 (10 min) and step 2 (10 min), DT, a fluorine free low-surface-energy molecule, was used to passivate the surface and the wettability was estimated. The surface displays superhydrophobicity ( $SCA = 165.1 \pm 2.4^\circ / SA = 4 \pm 1^\circ$ ) and oleophilicity with rapeseed oil/hexadecane ( $SCA \sim 10^\circ$ ). Such oleophilicity may be due to the fact that the surface energy of DT layer is larger than that of PFDT due to the different outermost group ( $-\text{CF}_3$  for PFDT,  $-\text{CH}_3$  for DT) and consequently the term  $\theta \geq 90^\circ$  (i.e.,  $\gamma_s \leq \gamma_l/4$ , see Introduction section) can not be obtained; according to the Wenzel model,<sup>16</sup> for  $\theta \leq 90^\circ$ , SCA is reduced with the increase of surface roughness and consequently oleophilicity is obtained. This phenomenon suggests that the outermost group influences the surface wettability greatly. To ensure the surface superoleophobicity in our present work, PFDT with  $-\text{CF}_3$  outermost group is quite needed.

**3.2.3. Stability.** Stability is the foundation of the potential applications for SHS or SOS. In this work, wear/humidity/UV/oxidation resistance for the sample fabricated by step 1 (10 min)/step 2 (10 min) were tested and the results were shown in Figure 4. For wear resistance, an abrasive paper (5000 mesh) was selected as friction mating, the applied load was 14 g, and the contact area is 15 mm  $\times$  15 mm (Figure 4a–i). It was observed that SCA decreased and SA increased as the sliding distance increasing. The critical sliding distance for the loss of superhydrophobicity ( $SCA > 150^\circ$  and  $SA < 10^\circ$ ) is found to be  $\sim 40$  cm, at that critical point, SCA and SA is  $164^\circ$  and  $9^\circ$ , respectively. For the probe liquid of hexadecane, a similar deterioration phenomenon is observed. However, because of

the lack of rigor about the SA for SOS (hexadecane), a clear critical point for the loss of superoleophobicity is difficult to point out. As the sliding proceeding to 4500 cm, for water and hexadecane, SCA/SA decrease finally to  $\sim 118^\circ/90^\circ$  and  $\sim 75^\circ/90^\circ$ , respectively. To discover the reason for the deterioration of SHS/SOS, digital pictures for the sample before (Figure 5a) and after (Figure 5b) sliding for 4500 cm was shown. It is obvious that the surface color changed greatly, suggesting that the outermost layer (i.e., PFDT) may be peeled off. SEM images showed that the nanorods were destroyed by the wear effect of the abrasive paper (compare Figure 5c and e or 5d and 5f) and obvious grooves (Figure 5f) were generated after sliding for 4500 cm. In others words, deterioration of SHS/SOS is due to the loss of PFDT and the change in surface morphology.

For humidity resistance, a self-made unit was used to evaluate the stability of the sample after placing in an environment with saturated water vapor. The results showed that, for both water and hexadecane probe liquids, as the treated time increasing, SCA decreased and SA increased, suggesting the loss of superhydrophobicity and superoleophobicity. The variation in morphology is not so obvious after the humidity resistance test (Figure 3s). So, such deterioration may be due to the desorption of PFDT species from the substrate under the attacking of water molecules. After the humidity resistance test, the sample was re-immersed into PFDT ethanol solution, and SCA/SA for water and hexadecane was measured to be  $166.5 \pm 1.5^\circ/4^\circ$  and  $156.5 \pm 2.5^\circ/18 \pm 4^\circ$ . These data suggest that superhydrophobicity and superoleophobicity can be recovered by PFDT re-modification and our assumption (i.e., deterioration may due to the desorption of PFDT) can be proved indirectly by such recovery. For UV resistance, during the test range, the change in wettability for water and hexadecane can be neglected. This suggests that both surface morphology (Figure 3s) and chemistry does not change greatly. For oxidation resistance, sample fabricated by step 1 (10 min)/step 2 (10 min) was placed in an atmospheric environment ( $25^\circ\text{C}$ , 45 % RH) for 10 days. After that, SCA/SA for water, and hexadecane, were measured to be  $167.5 \pm 1.5^\circ/4 \pm 2^\circ$ , and  $156.5 \pm 1.8^\circ/21 \pm 2^\circ$ , respectively. This implies the so-fabricated film is stable against oxidation under the testing conditions.

## 4. CONCLUSIONS

A convenient route, combining a two-step surface texturing process and succeeding surface passivation with low-surface-energy molecules, was proposed to fabricate SOS on copper substrate. It was discovered that the optimum surface structures for superoleophobicity with a combination of densely-distributed SMP and nano-rods can be obtained by controlling the treating time for step 1 (10 min) and step 2 (10 min); while, PFDT with an outermost  $-\text{CF}_3$  group is the ideal reagent to passivate the surface. This solution-immersion approach may accelerate the production of SOS (even with hexadecane, a typical low-surface-energy liquid) for its inherent advantages, such as the need of no special apparatus and relatively simple operation.

## ■ ASSOCIATED CONTENT

### 📄 Supporting Information

Surface morphologies for copper treated by step 1 for 15 and 20 min, surface morphology variation as treating time of step 2, and surface morphologies for the sample fabricated by step 1

(10 min)/step 2 (10 min) after humidity (168 h)/UV (10 days)/oxidation (10 days) resistance test. This material is available free of charge via the Internet at <http://pubs.acs.org>.

## AUTHOR INFORMATION

### Corresponding Authors

\*E-mail: [wenl@ualberta.ca](mailto:wenl@ualberta.ca). Tel.: +86-791-6453210. Fax: +86-791-6453210.

\*E-mail: [xuems04@mails.gucas.ac.cn](mailto:xuems04@mails.gucas.ac.cn)

### Notes

The authors declare no competing financial interest.

## ACKNOWLEDGMENTS

The authors acknowledge with pleasure the financial support of this work by the National Natural Science Foundation of China (Grants 21203089 and 51263018), and International S&T Cooperation Program of China (Grant 2012DFA51200).

## REFERENCES

- (1) Yang, Jin.; Zhang, Z. Z.; Xu, X. H.; Men, X. H.; Zhu, X. T.; Zhou, X. Y. *New J. Chem.* **2011**, *35*, 2422–2426.
- (2) Furstner, R.; Barthlott, W.; Neinhuis, C.; Walze, P. *Langmuir* **2005**, *21*, 956–961.
- (3) Mishchenko, L.; Hatton, B.; Bahadur, V.; Taylor, J.; A. Krupenkin, T.; Aizenberg, J. *ACS Nano* **2010**, *4*, 7699–7707.
- (4) Saito, H.; Takai, K.; Takazawa, H.; Yamauchi, G. *Mater. Sci. Res. Int.* **1997**, *3*, 216–219.
- (5) Liu, H. Q.; Szunerits, S.; Xu, W. G.; Boukherroub, R. *ACS Appl. Mater. Interfaces* **2009**, *1*, 1150–1153.
- (6) Ou, J. F.; Liu, M. Z.; Li, W. *Appl. Surf. Sci.* **2012**, *258*, 4724–4728.
- (7) Ou, J. F.; Hu, W. H.; Wang, Y.; Wang, F. J.; Xue, M. S.; Li, W. *Surf. Interface. Anal.* **2013**, *45*, 698–704.
- (8) Ou, J. F.; Hu, W. H.; Xue, M. S.; Wang, F. J.; Li, W. *ACS Appl. Mater. Interfaces* **2013**, *5*, 3101–3107.
- (9) Scardino, A. J.; Zhang, H.; Cookson, D. J.; Lamb, R. N.; de Nys, R. *Biofouling* **2009**, *25*, 757–767.
- (10) Chanyoung, J.; Chang-Hwan, C. *ACS Appl. Mater. Interfaces* **2012**, *4*, 842–848.
- (11) Saleema, N.; Sarkar, D. K.; R. Paynter, W.; Chen, X. G. *ACS Appl. Mater. Interfaces* **2010**, *2*, 2500–2502.
- (12) Xiang, M.; Jun, H. *Langmuir* **2009**, *25*, 11822–11826.
- (13) Archana, C.; Harish, C. B. *J. Phys. Chem. C* **2011**, *115*, 18213–18220.
- (14) Takahiro, I.; Michiru, S. *Langmuir* **2011**, *27*, 2375–2381.
- (15) Wu, W. C.; Wang, X. L.; Wang, D. A.; Chen, M.; Zhou, F.; Liu, W. M.; Xue, Q. J. *Chem. Commun.* **2009**, *9*, 1043–1045.
- (16) Wenzel, R. N. *Ind. Eng. Chem.* **1936**, *28*, 988–994.
- (17) Kaoru, T.; Takamasa, Y.; Tomohiro, O.; Satoshi, S. *Ind. Eng. Chem.* **1997**, *36*, 1011–1012.
- (18) C, W.; Extrand. *Langmuir* **2002**, *18*, 7991–7999.
- (19) Ahuja, A.; Taylor, J.A.; Lifton, V.; Sidorenko, A. A.; Salamon, T. R.; Lobaton, E. J.; Kolodner, P.; Krupenkin, T. N. *Langmuir* **2008**, *24*, 9–14.
- (20) Shreerang, S.; Chhatre; Wonjae, C.; Anish, T.; Kyoo-Chu, P.; Joseph, M.; Gareth, H.; McKinley; Robert, E. *Langmuir* **2010**, *26*, 4027–4035.
- (21) Cao, L.; Tyler, P.; Michael, W.; Gao, D. *Langmuir* **2008**, *24*, 1640–1643.
- (22) Yang, J.; Zhang, Z. Z.; Men, X. H.; Xu, X. H.; Zhu, X. T. *New J. Chem.* **2011**, *35*, 576–580.
- (23) Ellinas, K.; Tserepi, A.; Gogolides, E. *Langmuir* **2011**, *27*, 3960–3969.
- (24) Darmanin, T.; Guittard, F.; Amigoni, S.; Givenchy, E.T.; Noblin, X.; Kofman, R.; Celestini, F. *Soft Matter* **2011**, *7*, 1053–1057.
- (25) Cassie, A. B. D.; Baxter, S. *Trans. Faraday Soc.* **1944**, *40*, 546–551.
- (26) Milne, A. J. B.; Amirfazli, A. *Adv. Colloid Interface Sci.* **2012**, *170*, 48–55.
- (27) Takashi, F.; Yoshitaka, A.; Hiroki, H. *Langmuir* **2011**, *27*, 11752–11756.
- (28) Hong, Z.; Kock, Y. L.; Varun, S. *Langmuir* **2011**, *27*, 5927–5935.
- (29) Zhang, W.; Wen, X.; Yang, S.; Berta, Y.; Wang, Z. L. *Adv. Mater.* **2003**, *15*, 822–825.
- (30) Cudennec, Y.; Lecerf, A. *Solid State Sci.* **2003**, *5*, 1471–1474.
- (31) Whelan, C. M.; Kinsella, M.; Ho, H. M.; Maex, K. J. *Electron. Mater.* **2004**, *33*, 1005–1011.
- (32) Fonder, G.; Laffineur, F.; Delhalle, J.; Mekhalif, Z. *J. Colloid Interface Sci.* **2008**, *326*, 333–338.
- (33) Dilimon, V. S.; Denayer, J.; Delhalle, J.; Mekhalif, Z. *Langmuir* **2012**, *28*, 6857–6865.
- (34) Qian, B. T.; Shen, Z. Q. *Langmuir* **2005**, *21*, 9007–9009.
- (35) Liu, T.; Chen, S. G.; Cheng, S.; Tian, J. T.; Chang, X. T.; Yin, Y. S. *Electrochim. Acta* **2007**, *52*, 8003–8007.